ELSEVIER

International Journal of Mass Spectrometry 212 (2001) 205–217

www.elsevier.com/locate/ijms

# Application of the numerical model describing analyte permeation through hollow fiber membranes into vacuum for determination of permeation parameters of organic compounds in a silicone membrane

Alexey A. Sysoev[a]*, Raimo A. Ketola[b], Ismo Mattila[b], Virpi Tarkiainen[b], Tapio Kotiaho[b,c]*

[a]*Moscow State Engineering Physics Institute (Technical University), Kashirskoe sh. 31, Moscow 115409, Russia*
[b]*VTT Chemical Technology, P.O. Box 1401, FIN-02044 VTT, Espoo, Finland*
[c]*University of Helsinki, Department of Pharmacy, Viikki Drug Discovery Technology Center (DDTC), P.O. Box 56, FIN-00014 University of Helsinki, Finland*

Received 30 September 2000; accepted 7 April 2001

**Abstract**

Permeation parameters of several organic compounds were determined with a numerical simulation model developed earlier. Diffusivities were determined by calculating permeation curves at various diffusivity values and searching for a value of diffusivity that gave the best correlation of the theoretical curve with the experimental permeation curves. The method also allows determination of error in diffusivity calculation. Error is mainly caused by scattering of experimental data and adding organic interaction with a polymer into the character of a permeation curve. Gas phase distribution ratios were determined from literature data, and permeation selectivities were derived from comparison of experimental data measured by Membrane Inlet Mass Spectrometry (MIMS) and direct inlet measurements. Finding the highest concentration in gas and liquid phase at which the signal still behaves linearly allows estimation of the highest point of linear partitioning. The highest concentration at which diffusivity still remains constant can be estimated by finding the point at which the errors caused by the scattering of the experimental data and the contribution of organic interaction with a polymer into character of a permeation curve are equal. The model was postulated to be applicable over a concentration range in which membrane transport obeys ideal diffusion law, and there is linear sample/membrane partitioning. Calculated membrane diffusivities, water diffusivities, and water/membrane distribution ratios from literature sources were used to simulate permeation fluxes of organic compounds from aqueous phase as a function of the sample flow rate. Comparison of the simulated results showed generally good agreement with the experimental ones, and the expected behavior of permeating flux as a function of sample flow rate was observed. (Int J Mass Spectrom 212 (2001) 205–217)


## 1. Introduction

Membrane inlet mass spectrometry is a well-established analytical technique that has become increasingly popular in recent years [1–3]. Ultimate

* Corresponding authors. E-mail: tapio.kotiaho@helsinki.fi; alexey.sysoev@msl.mephi.ru

Dedicated to R. Graham Cooks on the occasion of his sixtieth birthday.

1387-3806/01/$20.00 
*PII* S1387-3806(01)00440-7

sensitivity and information richness of the method, together with direct rapid sampling, has resulted in an increasing number of new applications and the appearance of new MIMS-related methods [1–9]. Emerging applications require better understanding and correct description of membrane sampling processes. The problem of non–steady state permeation of compounds from a sample through a polymer membrane into vacuum can be solved analytically only for the simplest cases [10] and generally requires numerical simulation. During recent years, several analytical [11–13] and numerical [11,14–16] models describing non–steady state processes taking place in MIMS-related methods have been reported. Most of them use the solution-diffusion model [17,18]. It is presumed that analyte transport through a polymer membrane obeys Fick's laws 1 and 2 and that analyte partitioning at sample/membrane interfaces has a linear character (obeys Henry's law for gas samples and Nernst's law for liquid samples). It is also assumed that diffusivity and partitioning coefficients in both gas and liquid phase are concentration independent. However, for simulation of real processes, it is important to know the concentration ranges in which these models work satisfactorily and the reliability of diffusion parameters.

Watson and Payne have experimentally shown how a permeant concentration in a water solution determines both the concentration within the membrane and the diffusivity in the membrane for relatively high concentrations [19]. As the organic concentration in the aqueous feed solution increases over the molar fraction range 0.01–0.5, the organic separation factor falls dramatically and the membrane diffusivities of alcohols clearly rise.

In this article, the concentration ranges in which the numerical model we developed [16] and described in detail [20] can be used for simulation of permeation processes are reported. The use of the model for determination of permeation parameters for some compounds is also presented. The following three criteria were chosen to find ranges of concentrations over which the solution-diffusion model is applicable: first, ideality of the permeation curve. Both the rise time and fall time of the non–steady state permeation curve are mainly dependent on the diffusivity of a compound. Therefore, direct comparison of experimental permeation curves at different concentration levels with calculated ideal curves allows us to define the highest concentrations at which the diffusion can be considered to be ideal—the diffusion critical concentration. Strong nonlinearity of analyte partitioning at the sample/membrane interface can also distort permeation curves from ideality, but the effect of this factor is expected to be less significant.

Second, linearity of response for gas samples. Henry's law assumes that there is a linear dependence between concentrations in membrane phase and gas phase at a sample/membrane interface and that the distribution coefficient is concentration independent. Therefore, determination of linearity of response for gas phase analysis allows determination of the highest concentration at which sample/membrane analyte partitioning can be considered to be ideal—the gas/membrane partitioning critical concentration.

Finally, linearity of response for liquid samples. Nernst's law proposes that there is a linear dependence between concentrations in membrane phase and liquid phase at a sample/membrane interface and that the distribution coefficient is concentration independent. Therefore, determination of linearity of response for liquid phase analysis allows determination of the highest concentration at which sample/membrane analyte partitioning can be considered to be ideal—the liquid/membrane partitioning critical concentration.

These criteria cannot be considered to be independent. However, for every compound, it is possible to determine the range of concentration over which all these criteria are satisfied, and this range of concentration can be considered to be the range in which the numerical model developed [16,20] is applicable.

## 2. Experimental

The mass spectrometer used was a Balzers Omnistar quadrupole mass spectrometer (Balzers, Liecht-

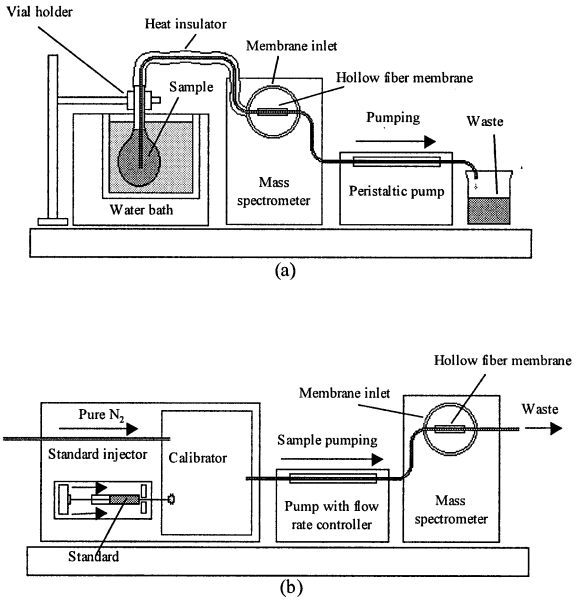


Fig. 1. A schematic picture of the experimental set-up used in (a) liquid phase MIMS experiments and (b) gas phase MIMS experiments.

enstein) with mass range of 1–300 U, equipped with a customized closed electron-impact (70 eV) ion source. Customizing the ion source was done by drilling holes to the ion source to make ionization chamber more open. A custom-made capillary flow-through membrane inlet was used. The temperature of the membrane inlet was 38°C. The membrane used in the study was Silastic silicone medical-grade tubing from Dow Corning (Midland, MI) with the following dimensions: inside diameter 0.0635 cm, outside diameter 0.1194 cm, length 0.8 cm. All the experiments were performed using selected-ion-monitoring mode (SIM) and an electron multiplier (SEM) for detection.

Fig. 1a shows the design of the experimental set-up used during analysis of liquid samples. A water stream is continuously supplied to a membrane inlet using a peristaltic pump (IPS4, Ismatec, Switzerland), and sample plugs are injected into this continuous water stream. Flow rates in the range of 0.5–10 mL/min were used. Samples were prepared in purified deionized water obtained using a Milli-Q academic A 10 (Millipore Corporation, Bedford, MA). The standard compounds were toluene [108-88-3] (99%), ethylbenzene [100-41-4] (99%) from Merck (Darmstadt, Germany), and ethanol [64-17-5] (99%) from Primalco Oy (Rajamäki, Finland). To minimize possible errors caused by variation of the sample temperature, the sample vials were placed in a water bath (Lauda M3, MGW, Germany) kept at 38°C and the sample lines were insulated with heat-insulating material.

The design of the experimental set-up used in the gas phase experiments is shown in Fig. 1b. Pure nitrogen (purity 99.999%, Oy AGA Ab, Espoo, Finland) from a gas cylinder was continuously supplied into the membrane inlet using a custom-made pump and flow-rate controller installed between the custom-made gas calibrator [21], used for gas sample preparation, and the membrane inlet. Gas samples were prepared in pure nitrogen (purity 99.999%, Oy AGA) and with 99% pure standards of benzene [71-43-2], toluene [108-88-3], ethylbenzene [100-41-4], methanol [67-56-1] from Merck, and ethanol [64-17-5] from Primalco Oy. Sample flow rate was 12 ml/min. The length of the sample line from the calibrator to membrane inlet of mass spectrometer was 1 m. For molar response coefficient determinations, a standard direct inlet from Balzers replaced the membrane inlet.

The diffusion critical concentrations and the diffusivities were determined by comparing the experimental permeation curves with those calculated using the numerical model [16,20]. The theoretical permeation curves were calculated, using various diffusivity values, with the same time step (typically 0.7 or 1.2 s/step) used for the experimental curves. In the next step of the data analysis, correlation coefficients for the simulated theoretical permeation curves and the experimental curves were calculated. The value of diffusivity corresponding to the maximum correlation was identified as a true diffusivity value. The average values reported are typically obtained on the basis of five repeated measurements at the same concentration level. There are two possible errors in the diffusivity determination—random and systematic. Random error is defined as unreproducibility of diffusion profile of a permeation curve caused by various kinds of fluctuations and random declining from ideal diffusion shape caused by mass spectrometric noise. Systematic declining of the experimental permeating

curve from the ideal shape causes systematic error of diffusivity determination. The decline is caused by organic interactions with a polymer. The systematic error also can be caused by deviation from ideal step function of analyte concentration in the feed stream. The following situations deviate the sample plug from an ideal step function: first, the finite amount of time needed to replace the clean air sample with the air sample containing an analyte throughout the entire capillary, and second, the existence of a finite interface layer between the clean air sample and the air sample containing analyte caused by diffusion of analyte molecules from the air sample containing the analyte into the clean nitrogen. The time needed to replace the clean air sample in membrane capillary for the current membrane geometry and 12 mL/min sample flow rate is 0.013 s. This time is negligible in comparison with the typical time of membrane diffusion. The time needed for a sample to come from the gas calibrator via the 100-cm length of the 0.2-cm-diameter transfer line to the capillary membrane is 16 s. For methanol, which has the highest air diffusivity of the studied compounds (diffusivity in air is 0.14 $cm^2/s$), this transfer time produces a 13-cm broadening of the characteristic interface layer. Because of the broad interface layer, it takes 2 s to replace the clean air sample with the air sample containing the analyte. This time is also negligible in comparison with the typical time for membrane diffusion. In conclusion, the systematic decline of the experimental permeating curve is mainly caused by organic interaction with the polymer. If systematic error is less than random error, then the permeation process is considered to be an ideal diffusion process. The diffusion critical concentration is the concentration at which the systematic error and random error of the diffusivity determination are the same. The diffusivity values determined at concentrations less than the critical ones present the best correlation between theoretical and experimental permeation curves and are considered to be the true values.

Gas/membrane partitioning critical concentration and liquid/membrane partitioning critical concentration were determined by measuring linearity of response for gas and liquid phase samples. Membrane permselectivities and gas/membrane distribution ratios were determined on the basis of the method described in the literature [22,23].

## 3. Results and Discussion

### *3.1. Mathematical model*

In this study, the numerical model described earlier [20] has been used to simulate mass transfer processes through a mobile phase, in a membrane, and into the vacuum of a mass spectrometer. The model considers a hollow fiber membrane probe in which the sample in gaseous or liquid mobile phase is flowing inside the capillary. The outside surface of the capillary membrane is exposed to the vacuum of a mass spectrometer. The concentration of the analyzed compounds is supposed to be small enough that a solution-diffusion model [17,18] can be applied. The flux through the membrane is considered to be small compared with the flow rate of sample through the capillary membrane.

Because diffusivities of organic compounds in gaseous mobile phase are much greater than in the membrane, the model considers diffusion in gaseous mobile phase to be instantaneous. This means that the analyte concentration in gaseous mobile phase is coordinate independent and that the time dependence of the concentration is the same as for the sample coming into the capillary membrane. Diffusivities of organic compounds in liquid mobile phase are comparable with the ones in the membrane. This and poor mixing in the sample/membrane interface produces a layer of analyte depletion next to the sample membrane interface. Therefore, analyte concentration in liquid mobile phase depends on radial and axial coordinates. To find the mobile phase concentration map as a function of time, the differential equation of continuity with appropriate boundary conditions has to be solved using the finite difference method of numerical analysis [24]. Under applied conditions, the flow of liquids is laminar, mass transport in axial direction of mobile phase has convective character, and mass transport in radial direction of the mobile

phase has diffusion character. The membrane phase concentration map as a function of time is found numerically by solving the equation of the diffusion (Fick's second law) with appropriate boundary conditions. The Crank-Nicolson method [10] has been applied to solve the corresponding partial differential equations.

The Matlab-5 computer code [20] based on the model is able to produce a concentration map inside the mobile phase and in the membrane as a function of time. Flux values at the vacuum side of the membrane can also be calculated as a function of time. The model allows us to simulate any measurement sequence and to simulate all the possible conversions between non–steady state processes by defining the time dependence of the concentration of the sample coming into a capillary membrane [20].

The best method to prove the correctness of the non–steady state permeation numerical model [16,20] is to compare results obtained with the model to the corresponding analytical solutions. The equation of non–steady state diffusion (Fick's second law),

$$\frac{\partial c}{\partial t} = D\,\frac{1}{r}\,\frac{\partial}{\partial r}\left(r\,\frac{\partial c}{\partial r}\right), \tag{1}$$

can be analytically solved for the cases when the concentration in the boundary layer of a mobile phase is changed by a step from 0 to $c^m$. The analytical solution for this example (reflecting the rise part of the permeation curves) derived from reference [10] will be

$$F(t) = \frac{2\pi\,L\,D\,K\,c^m(a)}{ln(b/a)} - 2\pi^2\,b\,L\,D\,K\,c^m(a) \cdot \sum_{i=1}^{\infty} \frac{J_0(b\alpha_n)\,J_0(a\alpha_n)\,U_1(b\alpha_n)}{J_0^2(b\alpha_n) - J_0^2(a\alpha_n)} \exp(-D\alpha_n^2\,t). \tag{2}$$

Here, $a$ and $b$ are the inner and outer radii of the membrane, respectively; $L$ is the membrane length; $D$ is diffusivity; $t$ is time; $J_i$, $Y_i$ are Bessel functions of the first and second kind, respectively, of order $i$; $\alpha_n$ is the roots of equation $U_0(a\alpha_n) = 0$, where

$$U_0(r\alpha_n) = J_0(r\alpha_n)\,Y_0(b\alpha_n) - J_0(b\alpha_n)\,Y_0(r\alpha_n);$$

$$U_1(b\alpha_n) = -\left.\frac{dU_0(r\alpha_n)}{dr}\right|_{r=b} = \alpha_n\,[J_1(b\alpha_n)\,Y_0(b\alpha_n) - J_0(b\alpha_n)\,Y_1 b\alpha_n)].$$

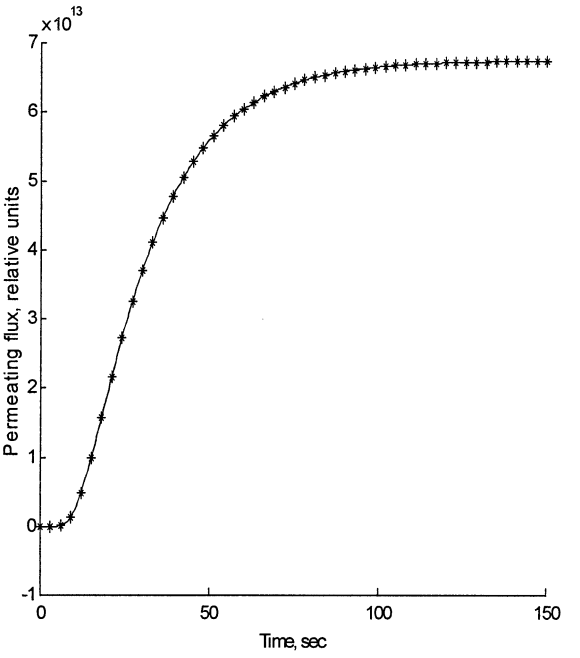


Fig. 2. Calculated permeation fluxes for $4.5 \times 10^{-11}$ moles/cm$^3$ toluene standard in nitrogen modulated by a step function. The solid line represents results of the analytical solution (calculated by formula [2]). Stars correspond to the results of the numerical solution of diffusion equations calculated using the developed numerical model [16,20].

A comparison example of the analytical and numerical solutions is presented in Fig. 2, which shows toluene permeation through a capillary membrane when the toluene concentration in nitrogen is instantaneously changed from 0 to a steady state level. Toluene diffusivity of 4.0 cm$^2$/s was used in the calculations. The solid line corresponds to the analytical solution (2) of the diffusion equation (1) calculated using the first 100 terms of the row. Stars

correspond to the numerical solution of the diffusion equation (1) calculated with a 0.1-s time step. The data calculated using the numerical model are in very good agreement with the data obtained using the analytical solution. The same excellent agreement was obtained for the data calculated for the case when the toluene concentration in nitrogen is instantaneously changed from a steady state level to 0. These findings prove that the numerical model developed [16,20] can be used for determination of diffusion constants.

### 3.2. Determination of diffusivities

Diffusivities for a selected set of compounds were determined by finding the correlation between experimental permeation curves and the curves obtained by the simulation. Two different kinds of block functions were used to modulate the sample stream. In the first case, fast sample modulation was used and the maximum permeating flux obtained during the sample introduction was ~50% of the steady state level. In the second case, prolonged sample modulation was used and the permeating flux had sufficient time to reach steady state level before the sample stream pumped through the inlet was changed to a continuous flow of pure nitrogen. These initial studies showed that prolonged sample modulation was less preferable for diffusivity determination. An example of this is presented in Fig. 3, which shows experimental permeating flux of toluene and a simulated solution for prolonged sample modulation at a concentration level of $4.5 \times 10^{-11}$ moles/cm$^3$. The theoretical permeation curve was calculated using a diffusivity value of $3.8 \times 10^{-6}$ cm$^2$/s, which corresponds to maximum correlation between the experimental and simulated permeation curves. Deviation of the experimental data from the diffusion law is quite significant and is especially evident as a nonideal top of the permeation curve. The response behavior observed is very similar to that reported by Lauritsen [13], and therefore, it is expected that, in this case also, the deviation of the experimental curve from ideality is caused by adsorption/desorption processes at vacuum surfaces of the mass spectrometer.

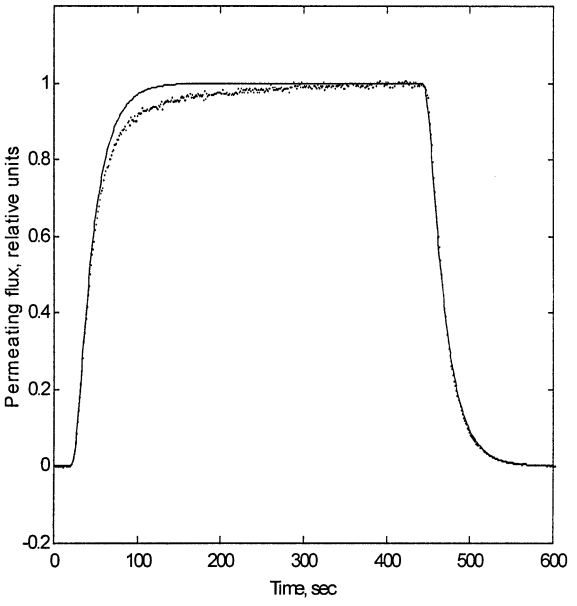


Fig. 3. Permeation fluxes for $4.5 \times 10^{-11}$ moles/cm$^3$ toluene standard in nitrogen modulated by 423-s block function. In the time of switch over, permeation flux reaches the steady state level. The dots correspond to the experimental values of permeating flux recorded with a 1.2-s step. The solid line corresponds to the results of simulations with a diffusivity value of 3.8 cm$^2$/s, a value that is in the best agreement with the experimental data presented.

The concentration dependency of the diffusivity determination was also studied. The shapes of experimental curves at low concentrations showed excellent accordance with the ideal diffusion law as demonstrated by Fig. 4, which shows experimental and simulated permeating flux for benzene ($4.5 \times 10^{-11}$ moles/cm$^3$ in $N_2$) measured using fast sample modulation. The theoretical permeation curve was obtained using a diffusivity value of $4.8 \times 10^{-6}$ cm$^2$/s, which corresponds to the maximum correlation with the experimental data. Deviation from the diffusion law is insignificant and is mainly caused by the noise of the mass spectrometer. Very good agreement was also obtained for all the experimental permeation curves for toluene, benzene, and ethylbenzene at concentrations $<9 \times 10^{-11}$ moles/cm$^3$ and with fast sample modulation. Relatively large scattering of experimental data for ethanol and methanol was observed at these levels of concentrations, presumably because of their higher detection limits. For the other com-

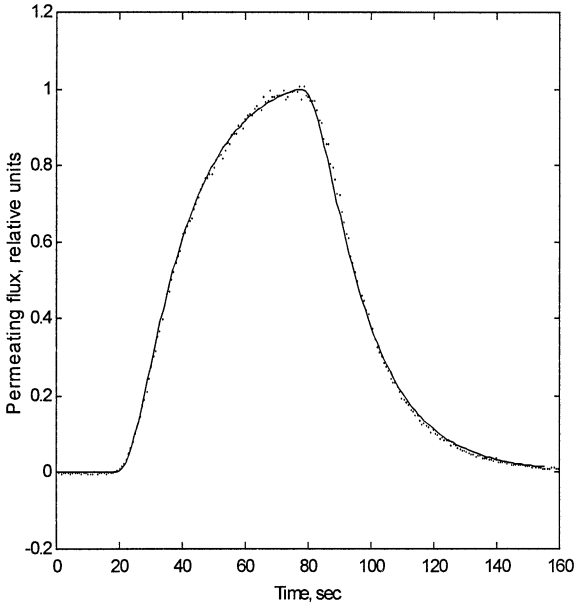


Fig. 4. Permeation flux for $4.5 \times 10^{-11}$ moles/cm$^3$ benzene standard in nitrogen modulated by 58-s block function. In the time of switch over, permeation flux reaches ~50% of the steady state level. The dots correspond to the experimental values of permeating flux recorded with a 0.7-s step. The solid line corresponds to the results of simulations with a diffusivity value of 4.8 cm$^2$/s, a value that is in the best agreement with the experimental data presented.

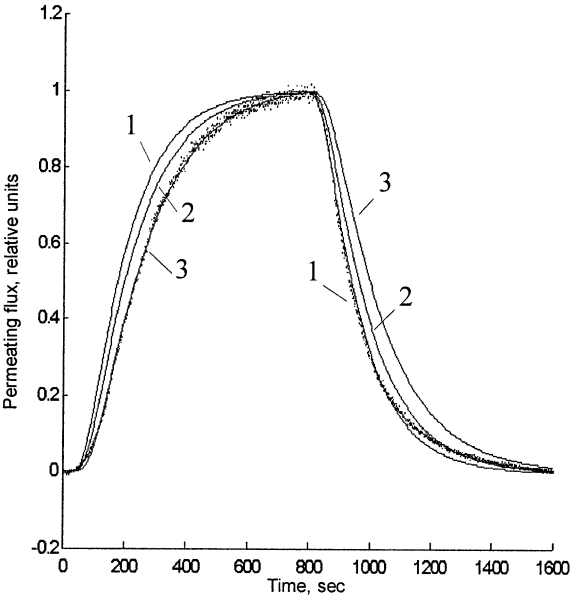


Fig. 5. Permeation for $9 \times 10^{-10}$ moles/cm$^3$ ethanol in nitrogen modulated by 763-s block functions. In the time of switch over, permeation flux reaches ~95% of the steady state level. The dots correspond to the experimental values of permeating flux recorded with a 1.2-s step. The solid lines correspond to results of simulations with a diffusivity value of (1) 0.6 cm$^2$/s, (2) 0.53 cm$^2$/s, and (3) 0.45 cm$^2$/s.

pounds, random error was the main source of error in these diffusivity determinations. However, at higher concentrations, the shapes of the experimental curves showed poorer agreement with the diffusion law above a critical concentration, which was different for each compound. Fig. 5 shows an experimental and three simulated permeating curves determined for $9 \times 10^{-10}$ moles/cm$^3$ ethanol sample in nitrogen. The rise part of line 3, calculated using a $0.45 \times 10^{-6}$ cm$^2$/s diffusion constant, is in the best accordance with the rise part of the experimental permeation curve and the fall part of line 1, calculated using a $0.6 \times 10^{-6}$ cm$^2$/s diffusion constant, is in the best accordance with the fall part of the experimental permeation curve. Line 2, calculated using a $0.53 \times 10^{-6}$ cm$^2$/s diffusion constant, corresponds to the intermediate value of diffusivity from these three theoretical lines. Systematic error caused by deviation from the ideal diffusion law is the main reason for the error of diffusivity determination, that is, ethanol permeation can not be described as ideal diffusion at this level of concentration.

The reported diffusivity values were calculated on the basis of the experimental permeation curves recorded at $4.5 \times 10^{-11}$ moles/cm$^3$ concentration (in $N_2$) of toluene, benzene, and ethylbenzene and at $4.5 \times 10^{-10}$ moles/cm$^3$ concentration (in $N_2$) of ethanol and methanol (Table 1).

The calculated diffusivities of alcohols are an order of magnitude smaller than the ones of aromatic hydrocarbons. Our data differ quite a lot from the data presented by Watson and Payne [19], who report diffusivities of alcohols and aromatic hydrocarbons to be the same order of magnitude. However, the absolute values of diffusivities obtained in the current study are in good agreement with the data presented in [23]. The diffusivities reported here differ from the values of LaPack et al. by the following amounts: 2% for benzene, 12% for toluene, 5% for methanol, 25% for ethylbenzene, and 47% for ethanol. LaPack et al.

Table 1
Measured, calculated, and literature parameters for the organic compounds used in the study

| Substance | Permselectivity (relative to $N_2$),$E$ | Diffusivity (experimental), D × $10^6$, $cm^2/s$ | Permeability, P × $10^6$, $\frac{cm^3\ cm}{s\ cm^2\ cm\ Hg}$ | Distribution ratio in $N_2$, $\frac{mole/cm^3}{mole/cm^3}$ | Distribution ratio in $H_2O$,[a] $\frac{mole/cm^3}{mole/cm^3}$ |
|---|---|---|---|---|---|
| Benzene | 491 | 4.8 ± 0.2 | 14 | 220 | 136 |
| Toluene | 1049 | 4.0 ± 0.2 | 29 | 560 | 346 |
| Ethylbenzene | 1796 | 3.2 ± 0.3 | 50 | 1200 | 847 |
| Methanol | 185 | 0.40 ± 0.02 | 5.2 | 990 | 29 |
| Ethanol | 141 | 0.53 ± 0.7 | 4 | 570 | 0.5 |

[a]Data from reference [26].

measured diffusivities [23] for silicon elastomer, composed of 69 wt% poly(dimetilsiloxane) and 31 wt% fumed silica (0.011-$\mu$m-diameter particles). Decrease of diffusive flow for the substances with greater hydrogen-bonding character was explained by the retention of the analyte by the highly polar silica filler. If permeant molecules interact only weakly with the polymer or filler, the diffusivity of a molecule is mainly dependent on the size of the molecule and less dependent on chemical properties. On the basis of these observations, it is concluded that the membrane used in this study is similar than the one used by LaPack et al. [23] and, therefore, similar diffusivities are obtained, but the membrane differs considerably from the one used by Watson and Payne [19].

### 3.3. Determination of selectivities and partitioning coefficients

Membrane/gas phase distribution ratios were determined for the studied compounds on the basis of the measured mass spectral data combined with literature data [25] and using the method of LaPack et al. [22,23].

Permselectivities (enrichment factor relatively to nitrogen) $E = P/P_{N_2}$ were determined from mass spectrometric response ratios and molar response factors using the following equation:

$$E = [I\gamma/I_{N_2}]\,[c^m_{N_2}/c^m]\,[M_{N_2}/M]^{1/2} \quad (3)$$

$I$ is a measured intensity of the monitored mass peak of the studied compound, obtained using membrane inlet. $I_{N_2}$ is a measured intensity of nitrogen (*m/z* 28 monitored), obtained using membrane inlet. $c^m$ is a concentration of the studied compound in gas mobile phase pumped through a membrane inlet. $c^m_{N_2}$ is a nitrogen concentration in gas mobile phase pumped through a membrane inlet. $M_{N_2}$ and $M$ are molecular weights of nitrogen and the studied compound, respectively, correcting discrimination caused by the reference direct inlet. Molar response factors, $\gamma$, were obtained from experimental data measured for the standard compounds using a direct inlet and were calculated by the formula

$$\gamma = \frac{c^d/I^d}{c^d_{N_2}/I^d_{N_2}}. \quad (4)$$

$c^d$ is a concentration of the studied compound in gas sample analyzed by direct inlet. $c^d_{N_2}$ is a nitrogen concentration in gas sample analyzed by direct inlet. $I^d$ is a measured intensity of the monitored mass peak of the studied compound. $I^d_{N_2}$ is a measured intensity of nitrogen (*m/z* 28 monitored). In this study, the most intensive signal of nitrogen does not exceed 2.5 × 10−8 A in MIMS measurements and 1 × 10−7 A in direct inlet measurements. Both values fall into the linear response range of SEM that was proved by a linearity measurement made for different compounds. This allows one to consider the influence of the SEM response to nonlinearity to be minimal. Accuracy of the determination of molar response factors could be improved using a Faraday cup detector.

Permeabilities were estimated from permselectivities (enrichment factor relative to nitrogen) and a

Table 2
Diffusion and mobile phase/membrane critical concentrations

| Substance | Diffusion critical concentration | | Gas/membrane partitioning critical concentration | | Liquid/membrane partitioning critical concentration | |
|---|---|---|---|---|---|---|
| | In contacting layer of membrane, mole/cm$^3$ | In gas phase, mole/cm$^3$ | In contacting layer of membrane, mole/cm$^3$ | In gas phase, mole/cm$^3$ | In contacting layer of membrane, mole/cm$^3$ | In liquid phase, mole/cm$^3$ |
| Benzene | $5 \times 10^{-7}$ | $2 \times 10^{-9}$ | $8 \times 10^{-9}$ | $4 \times 10^{-11}$ | $4 \times 10^{-7}$ | $4 \times 10^{-8}$ |
| Toluene | $1 \times 10^{-6}$ | $2 \times 10^{-9}$ | $2 \times 10^{-8}$ | $3 \times 10^{-11}$ | $4 \times 10^{-7}$ | $3 \times 10^{-8}$ |
| Ethylbenzene | $3 \times 10^{-7}$ | $2 \times 10^{-10}$ | $1 \times 10^{-7}$ | $9 \times 10^{-11}$ | $5 \times 10^{-6}$ | $3 \times 10^{-7}$ |
| Methanol | $2 \times 10^{-7}$ | $2 \times 10^{-10}$ | $3 \times 10^{-6}$ | $3 \times 10^{-9}$ | $2 \times 10^{-2}$ | $9 \times 10^{-4}$ |
| Ethanol | $3 \times 10^{-8}$ | $5 \times 10^{-11}$ | $1 \times 10^{-6}$ | $2 \times 10^{-9}$ | $3 \times 10^{-4}$ | $7 \times 10^{-4}$ |

Data for gas/membrane partitioning critical concentration were obtained from [28,29].

literature value for nitrogen permeability $P_{N_2}$ [25] using the following equation:

$$P = E \times P_{N_2}. \quad (5)$$

The gas phase distribution ratio $K$ was obtained from Henry's law's solubility coefficient $S$, total sample pressure $p_t$, and diffusivity $D$. Taking into account that $c = S \times p$, $c^m = p/p_t$, and $S = P/D$, where $p$ is a partial pressure of the substance in the sample, $K = c/c^m$ can be transformed [22] to the formula

$$K = P\, p_t/D, \quad (6)$$

used for gas phase distribution ratio determination.

Membrane/liquid phase distribution ratios (Table 1) were obtained from the literature [26]. The calculated values of permeability, permselectivity, and the gas/membrane distribution ratio are tabulated in Table 1.

The values of gas/membrane distribution ratios for the studied aromatic hydrocarbons are smaller than the ones published by Zhang and Pawliszyn [27] by a factor of 2.2, 2.4, and 2.7 for benzene, toluene, and ethylbenzene, respectively. Good agreement with the permselectivity values published in reference [23] was observed for all the studied compounds except for ethanol. The permselectivities reported here differ from the ones reported by LaPack et al. [23] by 2% for benzene, 9% for toluene, 16% for ethylbenzene, 0.5% for methanol, and 180% for ethanol. Similar agreement was observed for values of gas/membrane distribution ratio derived from the data published in reference [23]. The gas/membrane distribution ratios differ from the ones derived based on the data of LaPack et al. [23] by 4% for benzene, 3% for toluene, 40% for ethylbenzene, 0% for methanol, and 73% for ethanol. The good agreement is most probably explained by the similar composition of membranes used in reference [23] and in the current study.

### *3.4. Estimation of diffusion and mobile phase/membrane partitioning critical concentrations*

Diffusion critical concentrations for the selected compounds were estimated by analyzing reasons for the noncorrelation between the experimental and theoretical permeation curves. The diffusivity values reported in Table 1 were used in these determinations. Three experimental permeation curves were used for every compound at each studied concentration level. Random error of diffusivity determination was estimated from the data deviation. Systematic error of diffusivity determination was calculated as half of the difference between diffusivities that best describe the rise and the fall sections of a permeation curve. The concentration at which random error and systematic error are equal was defined as the diffusion critical concentration (see Table 2).

At a concentration higher than diffusion critical concentration, a permeation curve tends to deviate from the ideal diffusion profile because concentration dependence of diffusivity starts to occur. This is

apparent from the fact that the rise and the fall part of flux profile are described by different values of diffusivities. This phenomenon can be qualitatively explained, according to the above discussion and to Watson and Payne [19]. At low concentration, the majority of adsorption sites in polymer are unfilled, and diffusivity of the substances is defined by the interaction of the analyte molecules with adsorption sites. As the analyte concentration increases, an increasing number of these interaction sites tend to be filled, enabling subsequent permeant molecules to diffuse at a greater rate. At the beginning of permeation, process response is mainly defined by retention of analyte by adsorption sites. However, the beginning of the fall part of the permeation curve should reflect diffusion flow of large amount of analyte molecules that are significantly less retained by the adsorption sites. This means that diffusion constant determined by the rise part of the permeation curve should be less than diffusivity determined by the fall part of the same permeation curve. This explanation is in good agreement with the permeation curve of ethanol shown in Fig. 5. The tail of the dotted experimental permeation curve probably reflects diffusion flow of analyte molecules retained by the adsorption sites in the polymer. This mechanism is expected to be more pronounced for strongly interactive analytes. In particular, in silicone membrane with highly polar silica filler, diffusion-critical concentrations for alcohols are expected to be smaller than the ones for aromatic hydrocarbons, correlating with the results shown in Table 2.

Gas phase/membrane partitioning critical concentration and liquid phase/membrane partitioning critical concentration were found by measuring the upper limit of linearity of response for aqueous or gas phase (in $N_2$) standards of the selected compounds. The results obtained for liquid solutions are tabulated in Table 2. The data for gas samples were obtained from literature sources [28,29] and are shown in Table 2. Note that this approach is unable to define the concentration at which analyte–polymer interaction becomes significant. However, it does help to identify the concentration at which analyte–membrane interaction at the sample side does not prevent application of the model of linear partitioning for a particular membrane geometry.

Response deviation can be also associated with an effect of increasing pressure inside the customized closed ion source and nonlinear response of the electron multiplier. Nonlinearity caused by these two reasons is expected to have the same magnitude for all compounds having similar detection efficiencies. However, the MS responses of the analytes corresponding to the partitioning critical concentration differ a few orders of magnitude. The highest value of linear MS response signal corresponding to the liquid/membrane partitioning critical concentration of methanol was $2 \times 10^{-6}$ A. Even if this point of nonlinearity were explained by the effects mentioned, the other points of nonlinearity with significantly less response are expected to be caused by different reasons. In the same time, the calculated liquid/membrane partitioning concentrations for alcohols are in good agreement with the data presented in the work of Watson and Payne [19].

Membrane phase volume concentrations corresponding to all the critical concentrations were also calculated (Table 2). These concentrations represent concentrations in the surface layer of the membrane in contact with the mobile phase. For liquid/membrane partitioning critical concentration, the analyte depletion at the sample/membrane interface was taken into account. The numerical model [16,20] was used to calculate the concentration of analyte in the layer of mobile phase next to sample/membrane interface.

Both for the liquid and the gas samples, partitioning critical concentrations for alcohols are higher than for aromatic hydrocarbons. However, the diffusion critical concentration for ethanol is the lowest. Obviously, the lowest of the diffusion and the partitioning critical concentrations should be considered to be the highest concentration at which the solution-diffusion model is applicable. The values of gas/membrane critical concentration are the lowest ones for hydrocarbons. However, the values of diffusion critical concentration are the lowest ones for alcohols. The values of liquid/membrane critical concentration are higher than gas/membrane critical concentration both for hydrocarbons and for alcohols.

### 3.5. Liquid sample flow rate effect

Relative permeation fluxes of organic compounds from aqueous phase were simulated and measured experimentally at different sample flow rates to define correlation between the theoretical and experimental data and to test the validity of the model [16,20]. Values of the phase distribution ratio in $H_2O$ presented in Table 1 were obtained from literature sources [26]. The values of experimental permeating fluxes were derived from the relative intensities of the measured mass peaks subtracting the background signal and taking into account the molar response factors calculated by Eq. (4). The background signal is the measured intensity of the analyte ions monitored when clean water was pumped through the membrane inlet. The background signals measured at 0.5 mL/min sample flow rate were 13% of the $5.6 \times 10^{-8}$ mole/cm$^3$ toluene signal, 0.4% of the $5.6 \times 10^{-8}$ mole/cm$^3$ ethylbenzene signal, and 22% of the $5.6 \times 10^{-6}$ mole/cm$^3$ ethanol signal. The random noise for ethylbenzene and ethanol was a few orders of magnitude less than the background signal. Fig. 6 shows experimental and simulated permeation fluxes of toluene, ethylbenzene, and ethanol. The experimental dependence of ethanol varies insignificantly when the flow rate changes from 0.5 to 10 mL/min. The numerical model also obtains the same result. The relatively small value of the membrane/liquid phase distribution coefficient (see Table 1) for ethanol causes insignificant decrease of concentration in the depleted layer at the sample/membrane interface. Increasing the sample flow rate decreases the value of concentration drop at the sample/membrane interface and correspondingly increases the absolute value of concentration. However, for compounds with a low value of membrane/liquid phase distribution coefficient, the absolute value of concentration varies weakly and, therefore, the permeating flux of ethanol also varies weakly. In contrast to ethanol, the value of membrane/liquid phase distribution coefficient for toluene and ethylbenzene is relatively high (see Table 1), and the concentration drop in the depleted layer predicted by the model is rather significant, leading to clear dependence of the permeation flux on the sample flow rate. The overall shapes of the experimental and simulated curves are similar, but the experimental values of toluene and ethylbenzene fluxes increase fivefold, whereas the theoretical values of toluene and ethylbenzene fluxes increase only 2.5 times in the

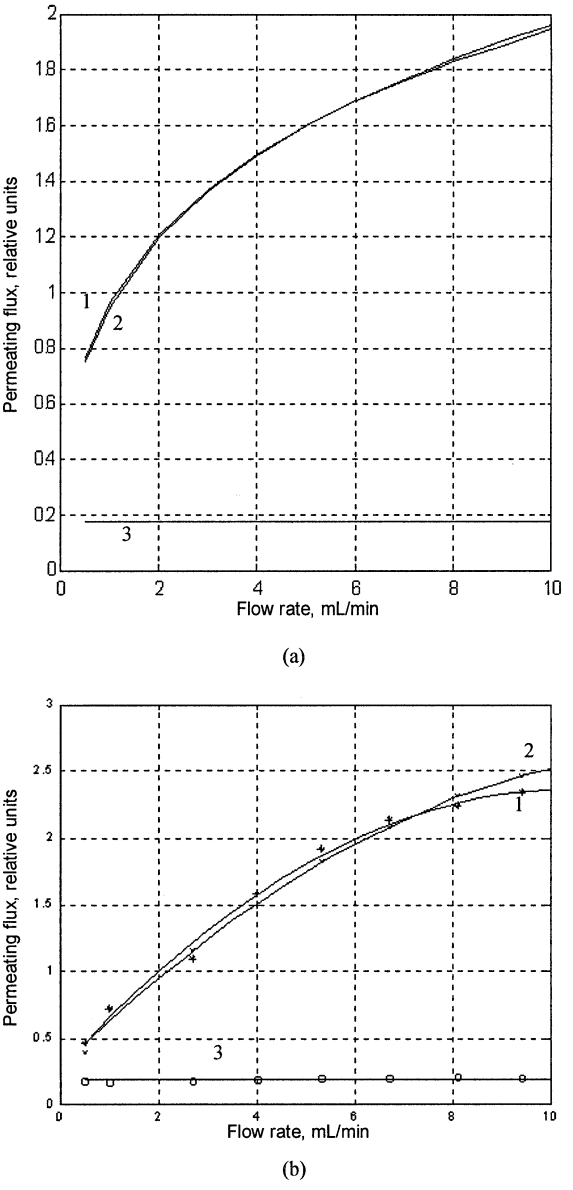


Fig. 6. (a) Theoretical and (b) experimental permeation fluxes for toluene (1), ethylbenzene (2), and ethanol (3) as a function of the liquid flow rate. Fluxes of toluene and ethylbenzene were studied at a concentration of $5.6 \times 10^{-8}$ mole/cm$^3$ and that of ethanol at $5.6 \times 10^{-6}$ mole/cm$^3$.

flow-rate range studied. The main reason for this discrepancy is thought to be some local turbulence of sample flow, which can occur because of the nonideal shape of the membrane lumen, caused by nonideal connections between the capillary membrane and the stainless steel tubing used to deliver the sample flow to the membrane and the reported bulking of the capillary membrane (F.R. Lauritsen, private communication) in the vacuum. Local turbulence can significantly improve mixing, decrease depleted layer thickness, and therefore, increase the permeating flux. This effect prevents use of the numerical model for the direct determination of liquid sample/membrane partition coefficients. At the same time, creating turbulent flow is an important factor of enhancing sensitivity of liquid-phase MIMS analysis of compounds with a relatively high membrane/liquid phase distribution coefficient.

## 4. Conclusion

The numerical model has been shown to allow determination of diffusion constants and to show the range where diffusivity can be considered concentration independent. Possible reasons for random error of diffusivity determination can be instrumental noise of the mass spectrometer, temperature fluctuations, and random membrane deformation caused by sample flow-rate instability. Systematic error of diffusivity determination is mainly caused by deviation from the ideal diffusion permeation flux versus time profile caused by interactions of the organic analytes with a polymer. Comparison of the contribution of these systematic and random errors makes it possible to define the concentration range in which the ideal diffusion model can be used. Determining the upper limit of the linearity range allows definition of gas/membrane and liquid/membrane critical concentrations. It was shown that the strongest limitation for the applicability of the solution-diffusion model is defined by the diffusion critical concentration for the studied alcohols and by gas/membrane critical concentration for the studied hydrocarbons. In addition, it was shown that, in general, the theoretical solutions calculated with the numerical model correlate very well with the experimental results.

## Acknowledgements

We are grateful to Timo Särme for his contribution to membrane inlet development. Sami Varjo is thanked for his assistance at the earlier stage of the work. Financial support by the Academy of Finland of the research of Alexey A. Sysoev is gratefully acknowledged.

## References

[1] T. Kotiaho, F.R. Lauritsen, T.K. Choudhury, R.G. Cooks, Anal. Chem. 63 (1991) 875A.
[2] F.R. Lauritsen, T. Kotiaho, Rev. Anal. Chem. 15 (4) (1996) 237.
[3] R.C. Johnson, R.G. Cooks, T.M. Allen, M.E. Cisper, P.H. Hemberger, Mass Spectrom. Rev. 19 (2000) 1.
[4] R. Kostiainen, T. Kotiaho, I. Mattila, T. Mansikka, M. Ojala, R.A. Ketola, Anal. Chem. 70 (1998) 3028.
[5] A.R. Dongre, M.J. Hayward, Anal. Chim. Acta 327 (1996) 1.
[6] M.A. Mendes, R.S. Pimpin, T. Kotiaho, M.N. Eberlin, Anal. Chem. 68 (1996) 3502.
[7] M.A. Mendes, R. Sparrapan, M.N. Eberlin, Anal. Chem. 72 (2000) 2166.
[8] F.R. Lauritsen, M.A. Mendes, T. Aggerholm, Analyst 125 (2000) 211.
[9] F.R. Lauritsen, J. Rose, Analyst 125 (2000) 1577.
[10] J. Crank, The Mathematics of Diffusion, 2nd edition, Clarendon, Oxford, 1975.
[11] G.-J. Tsai, G.D. Austin, M.J. Syu, G.T. Tsao, M.J. Hayward, T. Kotiaho, R.G. Cooks, Anal. Chem. 63 (1991) 2460.
[12] K.F. Hansen, S. Gylling, F.R. Lauritsen, Int. J. Mass Spectrom. Ion Processes 152 (1996) 143.
[13] F.R. Lauritsen, Int. J. Mass Spectrom. Ion. Processes 95 (1990) 259.
[14] F.L. Overney, C.G. Enke, J. Am. Soc. Mass Spectrom. 7 (1996) 93.
[15] F. Lennemann, Ph.D. Thesis, Hamburg-Harburg Technical University, Hamburg, 1999.
[16] A.A. Sysoev, Ph.D. Thesis, Moscow State Engineering Physics Institute (Technical University), Moscow, 1999.
[17] S.A. Stern, Membrane Separation Technology, Elsevier, Amsterdam, 1995.
[18] A.H.P. Skelland, Diffusional Mass Transfer, Wiley, New York, 1974.
[19] J.M. Watson, P.A. Payne, J. Mem. Sci. 49 (1990) 171.
[20] A.A. Sysoev, Anal. Chem. 72 (2000) 4221.
[21] R.A. Ketola, T. Mansikka, M. Ojala, T. Kotiaho, R. Kostiainen, Anal. Chem. 69 (1997) 4536.

[22] M.A. LaPack, J.C. Tou, C.G. Enke, Anal. Chem. 62 (1990) 1265.
[23] M.A. LaPack, J.C. Tou, V.L. McGuffin, C.G. Enke, J. Membrane Sci. 86 (1994) 263.
[24] A.A. Samarsky, J.P. Popov, Finite Difference Methods for Gas Dynamics, 3rd edition, Nauka, Moscow, 1992 (in Russian).
[25] W.L. Robb, Thin Silicone Membranes—Their Permeation Properties and Some Application, Report No. 65-C-031, October 1965, General Electric Research and Development Center, Schenectady, New York, p. 3.
[26] Yu Z. Luo, M. Adams, J. Pawliszyn, Analyst 122 (1997) 1461.
[27] Z.Zhang, J. Pawliszyn., Anal. Chem. 65 (1993) 1843.
[28] R.A. Ketola, M. Ojala, H. Sorsa, T. Kotiaho, R.K. Kostiainen, Anal. Chim. Acta 349 (1997) 359.
[29] T. Kotiaho, R.A. Ketola, M. Ojala, T. Mansikka, R. Kostiainen, American Environ. Lab. 3 (1997) 19.